

Theoretical study on the synthesis of methyl acetate from methanol and acetic acid in pervaporation membrane reactors: effect of continuous-flow modes

Suttichai Assabumrungrat^{a,*}, Jitkarun Phongpatthanapanich^a,
Piyasan Prasertthdam^a, Tomohiko Tagawa^b, Shigeo Goto^b

^a Department of Chemical Engineering, Research Center on Catalysis and Catalytic Reaction Engineering, Chulalongkorn University, Bangkok 10330, Thailand

^b Department of Chemical Engineering, Nagoya University, Chikusa, Nagoya 464-8603, Japan

Received 23 November 2002; accepted 15 March 2003

Abstract

The synthesis of methyl acetate (MeOAc) from methanol (MeOH) and acetic acid (HOAc) in pervaporation membrane reactors (PVMRs) is discussed in this paper. Three modes of PVMR operation, i.e. semi-batch (SB-PVMR), plug-flow (PF-PVMR) and continuous stirred tank (CS-PVMR) were modeled using the kinetic parameters of the reaction over Amberlyst-15 and permeation parameters for a polyvinyl alcohol (PVA) membrane). Both of the reaction and permeation rates are expressed in terms of activities. The PVA membrane shows high separation factors for HOAc and MeOAc but very low for MeOH. The simulation results of SB-PVMR mode show quite good agreement with the experimental results. The study focused on comparing PVMR performances between two modes of continuous-flow operation for various dimensionless parameters, such as Damkohler number (Da), the rate ratio (δ), the feed composition and the membrane selectivity. Flow characteristic within the reactors arisen from different operation modes affects the reactor performance through its influences on the reaction and permeation rates along the reactor. There are only some ranges of operating conditions where CS-PVMR is superior to PF-PVMR.

© 2003 Elsevier Science B.V. All rights reserved.

Keywords: Pervaporation membrane reactor; Methyl acetate synthesis; Activity coefficient; Simulation; Continuous operation

1. Introduction

In recent years, multifunctional reactors have attracted growing interest in both industrial and academic sectors. A number of reactors such as reactive distillation column, membrane reactor, pressure swing reactor and extractive reactor have been proposed to assist conversions of many chemical and biochemical reactions.

For esterification reactions which usually suffer from chemical equilibrium, most investigators have focused on applications of reactive distillation and membrane reactor. Pervaporation membrane reactor (PVMR) as one type of the membrane reactors combines chemical reaction and separation by pervaporation in a single unit. In the pervaporation,

one or more products (usually water) in a reaction liquid mixture contacting on one side of a membrane permeate preferentially through the membrane and the permeated stream is removed as a vapor from the other side of the membrane. As a result, the forward reaction can be enhanced. There are a number of reviews on pervaporation processes [1] and pervaporation combined with distillation and with chemical reactors [2,3]. Advantages of the PVMR are as follows: (a) the simultaneous removal of a product from the reactor enhances the conversion; (b) undesired side reactions can be suppressed; (c) the high conversion is possible at almost stoichiometric feed flow rates and (d) the heat of reaction can be used for separation. Therefore, lower capital investment, lower energy consumption and higher product yields make the pervaporation membrane reactor an interesting alternative to conventional processes.

PVMRs have been implemented in many reaction systems. Zhu et al. [4] studied the esterification reaction of acetic acid (HOAc) with ethanol both by experiment

Abbreviations: H₂O, water; HOAc, acetic acid; MeOH, methanol; MeOAc, methyl acetate

* Corresponding author.

E-mail address: suttichai.a@eng.chula.ac.th (S. Assabumrungrat).

Nomenclature

a_i	activity of species i
a'_i	modified activity of species i ($=K_i a_i / M_i$) (mol/kg)
A	membrane area (m^2)
Da	Damkohler number ($=k_1 W / F_{HOAc,0}$)
E_a	activation energy (J/mol)
F_i	molar flow rate of species i in the reaction side (mol/s)
\bar{F}_i	dimensionless molar flow rate of species i in the reaction side ($=F_i / F_{HOAc,0}$)
k_1	reaction rate constant (mol/(kg s))
K_e	equilibrium constant
K_i	adsorption parameter of species i
M_i	molecular weight of species i (kg/mol)
N_i	number of mole of species i in the reactor (mol)
P_i	permeability coefficient of species i (mol/(m^2 s))
Q_i	molar flow rate of species i in the permeate side (mol/s)
\bar{Q}_i	dimensionless molar flow rate of species i in the permeate side ($=Q_i / F_{HOAc,0}$)
r	reaction rate (mol/(kg s))
R_g	gas constant ($=8.314$ J/(mol K))
t	reaction time (s)
T	operating temperature (K)
W	catalyst weight (kg)
X_{eq}	equilibrium conversion
X_{HOAc}	conversion based on acetic acid

Greeks letters

α_i	separation factor of species i ($=P_{H_2O} / P_i$)
δ	rate ratio ($=P_{H_2O} A / k_1 W$)
ν_i	stoichiometric coefficient
ν	dimensionless axial coordinate
ξ	factor multiplying with the separation factors at $T = 323$ K

Subscript

0	initial value at $t = 0$
---	--------------------------

and simulation in a continuous-flow PVMR using a polymeric/ceramic composite membrane. Waldburger and Widmer [2] studied the same reaction in a continuous tube membrane (PVA) reactor. For the pervaporation-assisted process, a decrease of the energy input of over 75% and of the investment and operating costs of over 50% was estimated from the comparison of a conventional distillation process. Feng and Huang [5] studied an esterification reaction in a PVMR operated in the semi-batch mode and found that membrane permeability, membrane area and the volume

of the reaction mixtures are important operating parameters influencing the reactor behavior. Bagnell et al. [6] employed nafion tubes that function both as a reaction catalyst and a pervaporation membrane for the esterification of acetic acid with methanol (MeOH) and *n*-butanol. In the methanol reaction, the yield of methyl acetate (MeOAc) was increased from the usual equilibrium value of 73–77%. In the *n*-butanol reaction, the yield of *n*-butyl acetate increased from 70 to 95%. Okamoto et al. [7] studied the esterification of oleic acid with ethanol in the presence of *p*-toluenesulfonic acid using asymmetric polyimide membranes by simulation. The influence of operating parameters on the reaction time required for a conversion of 98% and on the productivity was investigated. Tanaka et al. [8] applied zeolite membranes to the esterification of acetic acid with ethanol. The studies were carried out by both experiment and simulation using a simple model based on the assumptions that the reaction obeyed second-order kinetics and the permeation flux of each component was proportional to its concentration. The influence of operating parameters on variation in conversion with reaction time was investigated by means of the simulation using the model. Liu and co-workers [9,10] studied on the esterification of acetic acid with *n*-butanol catalyzed by $Zr(SO_4) \cdot 4H_2O$ using cross-linked polyvinyl alcohol (PVA) membranes. Experiments and simulations were conducted to investigate the effects of several operating parameters, such as reaction temperature, initial molar ratio of acetic acid to *n*-butanol, ratio of the membrane area to the reacting mixture volume and catalyst concentration, on the PVMR. Domingues et al. [11] studied kinetics and equilibrium shift of a discontinuous esterification of benzyl alcohol with acetic acid using a commercial GFT membrane. A theoretical model was developed and the simulation results agreed well with the obtained experimental results. Xuehui and Lefu [12] modeled a semi-batch esterification process coupled by pervaporation and established a new method for measuring model parameters. Our previous work considered the synthesis of ETBE from TBA and EtOH in PVMR operated in the semi-batch mode [13].

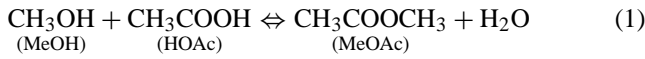
It should be noted that a model of a plug-flow pervaporation membrane reactor has already been included in a recent book [14]. The same author also extended their modeling works to include other configurations such as continuously stirred, batch, recycle plug-flow, recycle continuously stirred and recycle batch pervaporation membrane reactors [15].

In this paper, the synthesis of methyl acetate from methanol and acetic acid is used as a reaction example for comparing the performances of PVMRs operated in plug-flow (PF-PVMR) and continuous stirred tank (CS-PVMR) modes. Mathematical models using kinetic parameters of the reaction over Amberlyst-15 and permeation data for a polyvinyl alcohol membrane are developed and effects of various operating parameters expressed as dimensionless groups are investigated.

2. Mathematical modeling

2.1. Kinetics of the reaction

The reaction taking place in the reactor can be summarized as follows:



The rate model and the kinetic parameters of the reaction over Amberlyst-15 are expressed as follows [16]:

$$r = \frac{k_1(a'_{\text{HOAc}}a'_{\text{MeOH}} - a'_{\text{MeOAc}}a'_{\text{H}_2\text{O}}/K_e)}{(a'_{\text{HOAc}} + a'_{\text{MeOH}} + a'_{\text{MeOAc}} + a'_{\text{H}_2\text{O}})^2}; \quad \text{with}$$

$$a'_i = \frac{K_i a_i}{M_i}, \quad k_1 = 8.497 \times 10^9 \exp\left(\frac{-60470}{R_g T}\right),$$

$$K_e = 7.211 \times 10^{-2} \exp\left(\frac{3260}{R_g T}\right) \quad (2)$$

and $K_{\text{HOAc}} = 3.15$, $K_{\text{MeOH}} = 5.64$, $K_{\text{MeOAc}} = 4.15$, $K_{\text{H}_2\text{O}} = 5.24$.

The activity (a_i) can be calculated using the UNIFAC method.

2.2. Rates of pervaporation

Assuming that partial pressure of all species in the permeate side was low, the permeation rate of species i through the membrane can be expressed as

$$Q_i = AP_i a_i \quad (3)$$

The relationship between the permeability coefficient and operating temperature can be correlated by the Arrhenius equation.

$$P_i = P_{i,0} \exp\left(\frac{-E_a}{R_g T}\right) \quad (4)$$

2.3. Modeling of pervaporation membrane reactors

Three operation modes of PVMRs, i.e. semi-batch (SB-PVMR), continuous stirred tank (CS-PVMR) and plug-flow (PF-PVMR) were considered in the study. The mathematical models were obtained from material balances around the reactors, assuming the reactors behaved ideally. In addition, isothermality, negligible pressure drop, negligible heat- and mass-transfer resistances aside from the permeation process and no coupling effect of mixtures on the permeability were assumed. The sets of equations for different operating modes can be summarized as follows:

$$\frac{d}{dt} N_i = v_i W k_1 \frac{a'_{\text{HOAc}} a'_{\text{MeOH}} - a'_{\text{MeOAc}} a'_{\text{H}_2\text{O}} / K_e}{(a'_{\text{HOAc}} + a'_{\text{MeOH}} + a'_{\text{MeOAc}} + a'_{\text{H}_2\text{O}})^2} - AP_i a_i \quad (\text{SB-PVMR}) \quad (5)$$

$$\frac{d}{dv} \bar{F}_i = v_i Da \frac{a'_{\text{HOAc}} a'_{\text{MeOH}} - a'_{\text{MeOAc}} a'_{\text{H}_2\text{O}} / K_e}{(a'_{\text{HOAc}} + a'_{\text{MeOH}} + a'_{\text{MeOAc}} + a'_{\text{H}_2\text{O}})^2} - \frac{Da \delta a_i}{\alpha_i} \quad (\text{PF-PVMR}) \quad (6)$$

$$\frac{d}{dv} \bar{Q}_i = \frac{Da \delta a_i}{\alpha_i} \quad (\text{PF-PVMR}) \quad (7)$$

$$\bar{F}_{i,0} - \bar{F}_i + v_i Da \frac{a'_{\text{HOAc}} a'_{\text{MeOH}} - a'_{\text{MeOAc}} a'_{\text{H}_2\text{O}} / K_e}{(a'_{\text{HOAc}} + a'_{\text{MeOH}} + a a'_{\text{MeOAc}} + a'_{\text{H}_2\text{O}})^2} - \frac{Da \delta a_i}{\alpha_i} = 0 \quad (\text{CS-PVMR}) \quad (8)$$

Various design operating parameters and physical property parameters are characterized in dimensionless groups to facilitate parametric analysis for the comparison of reactor performances under different operation modes.

- (1) Damkohler number, Da ($=k_1 W / F_{\text{HOAc},0}$) is a measure of the residence time.
- (2) The rate ratio, δ ($=P_{\text{H}_2\text{O}} A / k_1 W$) is a measure of the ratio between permeation rate and reaction rate.
- (3) The separation factor, α_i ($=P_{\text{H}_2\text{O}} / P_i$) is a measure of membrane selectivity.

Some of the above assumptions may not be valid in all ranges of operating conditions of the PVMRs. Coupling effects in liquid mixtures are known to have a significant impact on actual permeabilities. For PF-PVMR, the axial pressure drop can be significant at high Reynolds numbers and the mass-transfer resistance between the liquid bulk and the surface of catalyst particles and also of the membrane surface becomes significant at large value of Da . In addition, non-ideal conditions such as complete mixing in CS-PVMR; non-isothermal condition; radial and axial gradient of concentration and temperature, should exist in actual operation of both modes. More rigorous models should be investigated in future studies.

EQUATRAN-G (all-purpose equation solver, Omega Simulation Co. Ltd.) was employed to solve the equations.

Comparison between our models and models of Lim et al. [15] reveals that despite of different dimensionless terms, the models are based on the same fundamental. The models take into account the non-ideal effect by expressing the reaction and permeation rates in terms of the activities. The reactor is assumed to behave as an ideal reactor and the concentration polarization effect is considered negligible. In addition, the membrane is assumed to be completely unreactive.

However, our models are based on the experimental data of reaction rates and permeation rates.

3. Experimental

3.1. Materials

PVA membranes (PERVAP 2201) supplied by Sulzr Chemtech GmbH-Membrane Systems and Amberlyst-15

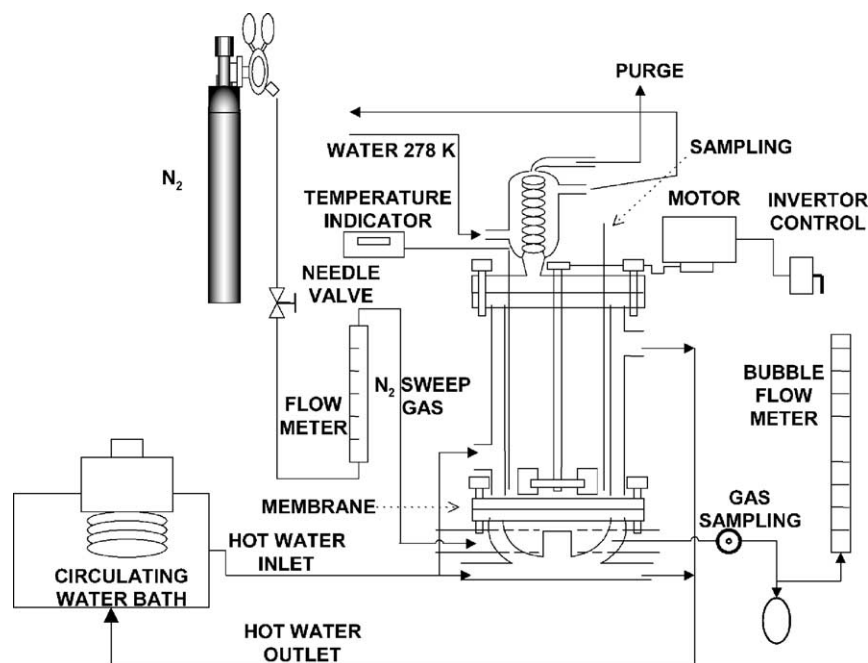


Fig. 1. Experimental apparatus.

obtained from Fluka were used as a water-selective membrane and a catalyst, respectively. Analytic grade methanol (MeOH) and acetic acid (HOAc) were used in the study.

3.2. Permeation study

Fig. 1 shows a schematic diagram of the pervaporation measurement apparatus. The PVA membrane with an effective area of 63 cm^2 was placed between two chambers. Hot water was circulated in jackets around the chambers to keep the system at a constant temperature. A disk turbine fully stirred a liquid mixture in the upper chamber while a condenser was attached to the system to condense all vapors leaving the reaction chamber. N_2 sweep gas at a constant molar flow rate of $8.9 \times 10^{-5} \text{ mol/s}$ was fed to the permeation side in the lower chamber to increase the driving force of the permeation. The molar flux of each species was obtained by measuring the exit volume flow rate and its composition by a bubble flow meter and a gas chromatography with a Gaskuropack 54 packed column, respectively. It should be noted that the concentration change in the liquid mixture could be neglected due to small amount of permeation compared to the amount of the liquid mixture.

3.3. Pervaporation membrane reactor studies

Experiments on the semi-batch pervaporation membrane reactor were carried out in the same apparatus for the permeation study; however, a frame of four catalyst baskets (as shown in Fig. 2) was mounted on the rotating shaft. The cylindrical baskets (i.d. = 2.5 cm and length = 6 cm) were

made of stainless steel screens. The catalyst, Amberlyst-15 (average diameter = 0.78 mm) was packed into the basket. The frame was held above the liquid level by upper hooks as shown in Fig. 2(a). After the nitrogen flow rate and temperature were maintained at desired values, the reaction was

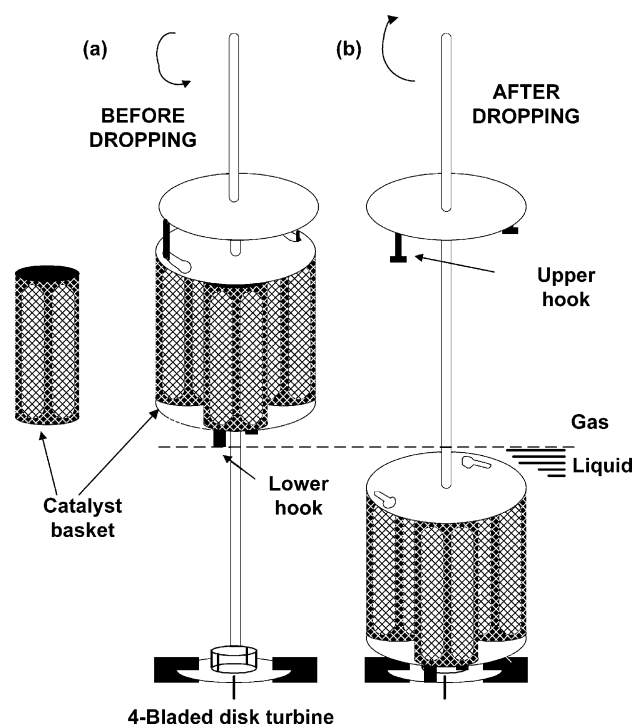


Fig. 2. Details of catalyst basket assembly: (a) before dropping and (b) after dropping.

started by changing the direction of agitation so that the frame of baskets dropped into the liquid mixture and, hence, an accurate start-up time can be determined [17]. The lower hooks were securely connected with slots on the disk turbine and the frame was rotated without slip as shown in Fig. 2(b). The stirring speed was fixed at the highest speed of 1210 rpm to reduce external mass-transfer resistance.

4. Results and discussion

4.1. Permeation studies

Table 1 summarizes the liquid mole fraction, liquid activity, permeability coefficients and separation factors for the permeation experiments of quaternary mixtures (H₂O–MeOH–HOAc–MeOAc) at three temperature levels. It was found that the permeation of acetic acid is negligibly small whereas methanol can permeate through the membrane at significant rate and, hence, the separation factor of methanol, α_{MeOH} , was low. Increasing the temperature results in the decrease of the separation factors. This behavior is observed in many other systems [18]. It should be noted that the expressions shown in terms of activity are more appropriate as the activity deviates significantly from ideality. The obtained permeability coefficients were fitted with good agreement with the Arrhenius equation (shown in Fig. 3) and the expressions are as follows:

$$P_{\text{H}_2\text{O}} = 2.01 \times 10^1 \exp\left(\frac{-3173}{T}\right) \quad (9)$$

$$P_{\text{MeOH}} = 2.92 \times 10^5 \exp\left(\frac{-6756}{T}\right) \quad (10)$$

$$P_{\text{MeOAc}} = 7.88 \times 10^7 \exp\left(\frac{-9385}{T}\right) \quad (11)$$

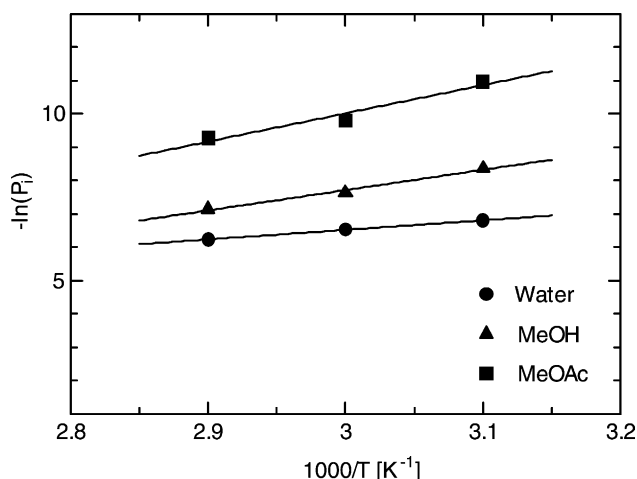


Fig. 3. Arrhenius plot of permeability.

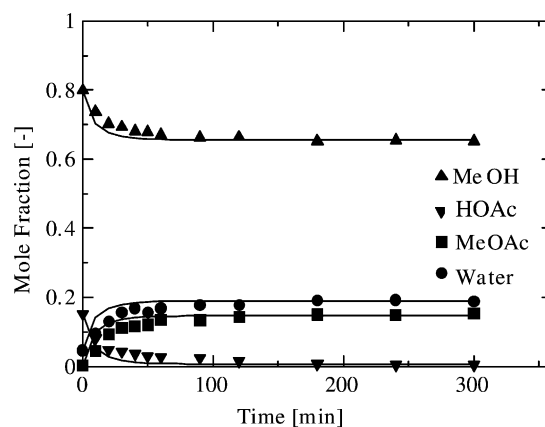


Fig. 4. Comparison between experimental and simulation results of SB-PVMR.

4.2. Pervaporation membrane reactor studies

Fig. 4 compares the experimental and simulation results of SB-PVMR. The initial moles of HOAc and MeOH were 1 and 5 mol, respectively, and the operating temperature was at $T = 333$ K. The model predicts the experimental results quite well. Discrepancy may be arisen from the deviation of permeability coefficients with compositions due to the interaction between components or from non-ideal behavior in the reactor. However, to simplify the model, this effect was neglected in the study.

4.3. Comparison between two modes of continuous operation

4.3.1. Effect of Damkohler number (Da)

Fig. 5 shows the effect of the Damkohler number (Da) on conversion (X_{HOAc}) at various values of the rate ratio (δ). The simulations were based on the values of separation factors (α_i) at $T = 323$ K and the stoichiometric feed ratio. The conversion (X_{HOAc}) is defined as follows:

$$X_{\text{HOAc}} = 1 - \frac{\bar{F}_{\text{HOAc}} + \bar{Q}_{\text{HOAc}}}{\bar{F}_{\text{HOAc},0}}$$

Increasing the values of Damkohler number (Da) increases residence time and, hence, higher conversions are achieved in both PF-PVMR and CS-PVMR modes. The rate ratio (δ) plays an important role on the performance of PVMR. The case with $\delta = 0$ represents conventional reactors whose maximum conversion is limited at an equilibrium value. At higher value of δ , it is possible to exceed the equilibrium conversion encountered in the conventional reactors. This is in agreement with experimental observations in other systems [4,19]. Comparing between two operation modes, it is found that PF-PVMR offers higher conversions than CS-PVMR.

4.3.2. Effect of rate ratio (δ)

Fig. 6 shows the effect of the rate ratio (δ) at 4 values of Damkohler number ($Da = 0.5, 1, 25$ and 75). There exists

Table 1
Feed composition, feed activity, permeability coefficients and separation factor at three temperature levels

Temperature (K)	Liquid mole fraction				Liquid activity				Permeability coefficient (mol/(m ² s))				Separation factor			
	Water	MeOH	MeOAc	HOAc	Water	MeOH	MeOAc	HOAc	Water	MeOH	MeOAc	HOAc	Water	MeOH	MeOAc	HOAc
323	0.1009	0.6748	0.0461	0.1782	0.1720	0.6724	0.0877	0.1672	1.11×10^{-3}	2.33×10^{-4}	1.73×10^{-5}	0	1.0	4.7	64	∞
333	0.1127	0.6617	0.0513	0.1743	0.1916	0.6612	0.0976	0.1670	1.45×10^{-3}	4.79×10^{-4}	5.49×10^{-5}	0	1.0	3.0	26	∞
343	0.1201	0.6378	0.0616	0.1804	0.2055	0.6396	0.1144	0.1758	1.96×10^{-3}	7.88×10^{-4}	9.35×10^{-5}	0	1.0	2.5	21	∞

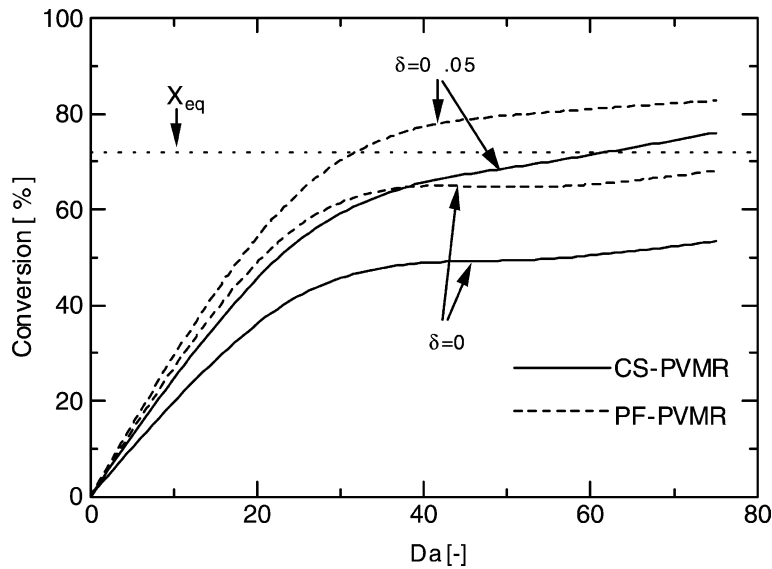


Fig. 5. Effect of Damkohler number (Da) on conversion.

an optimum rate ratio (δ), which provides a maximum conversion, for each value of Damkohler number (Da). Increasing the rate ratio (δ) at its low values is beneficial to the system due to the enhanced forward reaction from the removal of product H_2O ; however, the effect of reactant loss retards the improvement at high values of the rate ratio (δ) as shown in Fig. 7 for $Da = 25$. The presence of an optimum rate ratio was observed in another system for ethyl acetate production in both PF-PVMR and CS-PVMR modes [15].

Loss of component in y-axis (Fig. 7) represents the value of $\bar{Q}_i/\bar{F}_{HOAc,0}$. The superiority among PF-PVMR and CS-PVMR in term of maximum obtainable conversion was obviously dependent on the value of Damkohler number

(Da). At low value, CS-PVMR is superior to PF-PVMR; however, the opposite results are observed at higher values. It should be noted that the results reported by Lim et al. [15] only indicate the range where PF-PVMR shows a superior performance than CS-PVMR.

Differences in reactor performances between two operation modes are arisen mainly from the different flow characteristics within the reactors. In CS-PVMR, due to well-mixed condition, the reactant concentrations are at their lowest values and, consequently, the reaction takes place at its lowest rate. However, when considering the separation point of view, the well-mixed condition may be beneficial to the system. Because the product concentrations

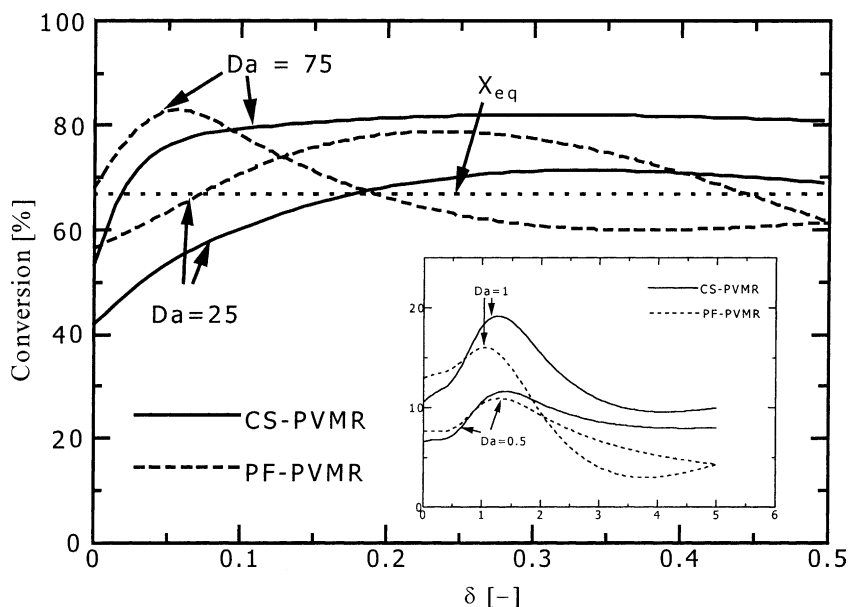


Fig. 6. Effect of rate ratio (δ) on conversion.

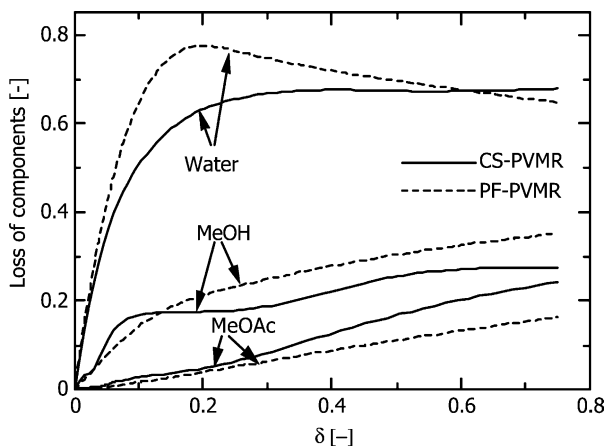


Fig. 7. Effect of rate ratio (δ) on reactant/product losses for $Da = 25$.

especially H_2O and the reactant concentrations are at their highest and lowest values, respectively, the entire membrane is efficiently utilized for product removal and, in addition, the reactant losses are at the smallest rates. Considering PF-PVMR, the plug-flow condition usually allows the reaction to proceed at higher extent compared to the well-mixed condition due to high reactant concentrations near the reactor entrance; however, it leads to high reactant losses and low product removal at the initial section. In short, the different flow characteristics within the reactors under different operation modes affect the performance of PVMRs via the effects on the rates of reaction and separation.

At low Damkohler number ($Da = 0.5$ and 1), CS-PVMR is superior to PF-PVMR. Because the residence time is small, the reaction proceeds at small extent. The effect of H_2O removal on enhancing forward reaction in CS-PVMR is higher than PF-PVMR due to the efficient utilization

of membrane area. However, at higher Damkohler number (Da), the increasing reaction rate in PF-PVMR predominates. The reaction moves forward at higher extent and the H_2O removal is high near the end of the reactor. As a result, PF-PVMR is superior to CS-PVMR. It is noted that it is desirable to operate the reactor at high conversion so PF-PVMR seems to be a favorable mode in a practical operation. In addition, the optimum rate ratio (δ) of CS-PVMR is always higher than that of PF-PVMR, indicating that CS-PVMR requires higher membrane area than PF-PVMR.

4.3.3. Effect of feed composition

Since MeOH permeates through the membrane at significant rate, it is likely to operate the reactor with feed composition of MeOH higher than the stoichiometric value. Fig. 8 shows the effect of feed composition on the maximum conversion at $Da = 25$ and 75 . The maximum conversion was determined by varying the values of the rate ratio (δ) as illustrated in the previous section. It was found that the optimum feed ratio (MeOH/HOAc) is approximately 1.8. Higher feed ratio results in the decreased feed concentration and reaction rate; however, at feed ratio lower than the optimum value the effect of reactant loss limits the conversion.

4.3.4. Effect of membrane selectivity

Fig. 9 shows the effect of membrane selectivity on the conversion for $Da = 25$. ξ is defined as the factor multiplying with the separation factors at $T = 323$ K. It is found that for $\xi = 1$, at high values of the rate ratio (δ) the conversion decreases with the increase of the rate ratio (δ) due to the effect of reactant loss (as shown in Fig. 10). There is no significant improvement when ξ increases from 10 ($\alpha_{MeOH} = 47$) to 100 and 1000 ($\alpha_{MeOH} = 470$ and 4700).

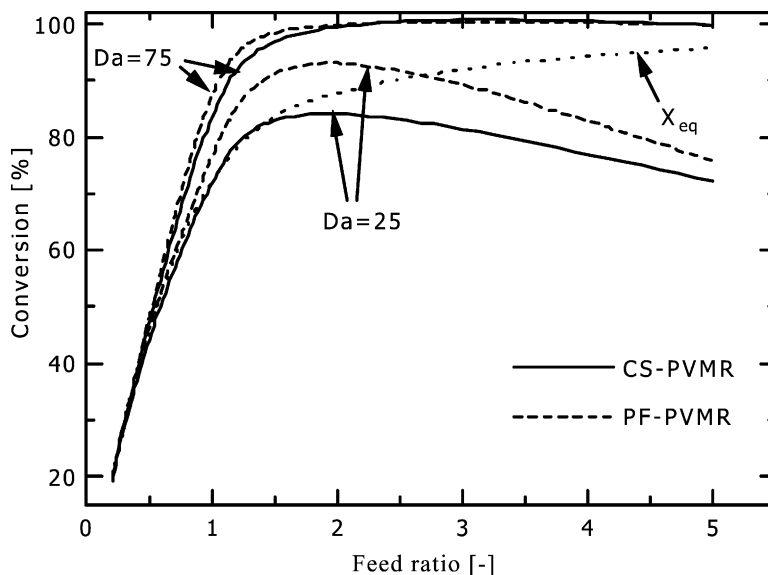


Fig. 8. Effect of feed composition on conversion.

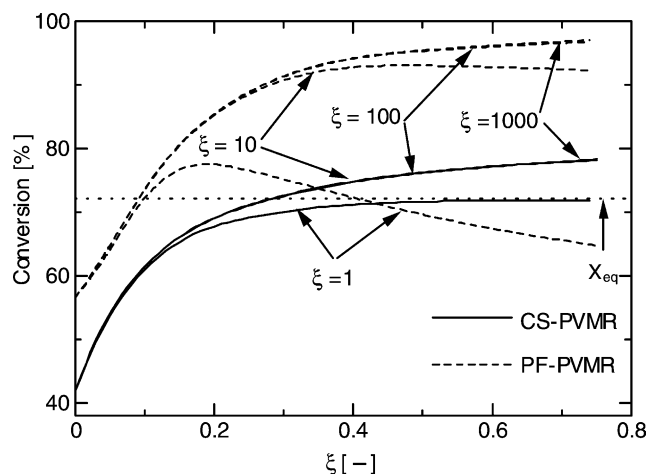


Fig. 9. Effect of membrane selectivity on conversion.

Further simulations of PF-PVMR reveals that at $\delta = 0.75$, membranes with $\alpha_{\text{MeOH}} = 47, 141$ and 188 are enough to offer the conversions of $95.0, 98.8$ and 99.2% , respectively, of that obtained when $\alpha_{\text{MeOH}} = 4700$, indicating that there is a range of membrane selectivity which plays an important role on the reactor performance. Again, it is observed that the maximum obtainable conversion of PF-PVMR is superior to that of CS-PVMR at higher membrane selectivity.

Loss of methanol in y -axis (Fig. 10) represents the value of $\bar{Q}_{\text{MeOH}}/\bar{F}_{\text{HOAc},0}$. For $\xi = 1$, at high values of the rate ratio (δ) the loss of methanol in PF-PVMR is higher than that in CS-PVMR. However, at higher ξ ($=100, 1000$), the loss of methanol becomes negligible. Therefore, the selection of pervaporation membrane with higher separation factor of methanol to water is required.

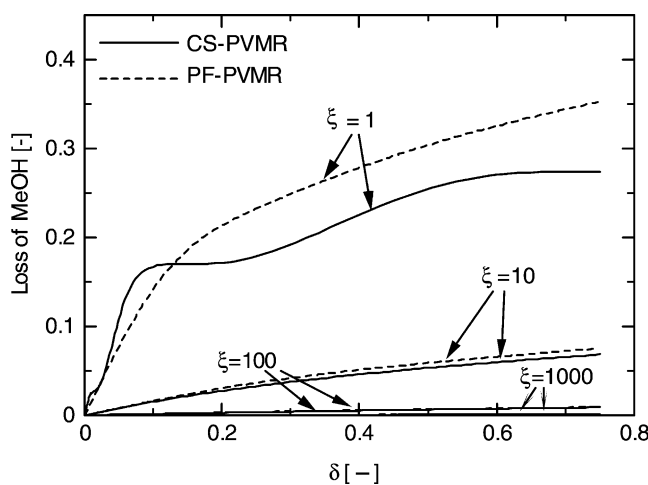


Fig. 10. Effect of membrane selectivity on MeOH loss.

5. Conclusion

Modeling of the esterification of acetic acid with methanol in the pervaporation membrane reactors demonstrates the following:

- PF-PVMR is a favorable mode although there are some ranges of operating conditions where CS-PVMR is superior to PF-PVMR.
- Flow characteristic in the reactor arisen from different mode affects the reactor performance through its influences on the reaction and permeation rates along the reactor.
- A membrane with high selectivity is essential for PVMR to achieve high reactor performance.

Acknowledgements

The research is supported by the Thailand Research Fund and TJTTP-JBIC. The authors also would like to thank Miss Wichitra Boonsiri for her technical help.

References

- B.K. Dutta, W. Ji, S.K. Sikdar, *Sep. Purif. Methods* 25 (1996) 131–224.
- R.M. Waldburger, F. Widmer, *Chem. Eng. Tech.* 19 (1996) 117–126.
- F. Lipnizki, R.W. Field, P.K. Ten, *J. Membr. Sci.* 153 (1999) 183–210.
- Y. Zhu, R.G. Minet, T.T. Tsotsis, *Chem. Eng. Sci.* 51 (1996) 4103–4113.
- X. Feng, R.Y.M. Huang, *Chem. Eng. Sci.* 51 (1996) 4673–4679.
- L. Bagnell, K. Cavell, A.M. Hodges, M.A.T. Seen, *J. Membr. Sci.* 85 (1993) 291–299.
- K. Okamoto, M. Yamamoto, Y. Otoshi, T. Semoto, M. Yano, K. Tanaka, *J. Chem. Eng. Jpn.* 26 (1993) 475–481.
- K. Tanaka, R. Yoshikawa, C. Ying, H. Kita, K. Okamoto, *Catal. Today* 67 (2001) 121–125.
- Q.L. Liu, Z. Zhang, H.F. Chen, *J. Membr. Sci.* 182 (2001) 173–181.
- Q.L. Liu, H.F. Chen, *J. Membr. Sci.* 196 (2002) 171–178.
- L. Domingues, F. Recasens, M.A. Larrayoz, *Chem. Eng. Sci.* 54 (1999) 1461–1465.
- L. Xuehui, W. Lefu, *J. Membr. Sci.* 186 (2001) 19–24.
- W. Kiatkittipong, S. Assabumrungrat, P. Praserttham, S. Goto, *J. Chem. Eng. Jpn.* 35 (2002) 547–556.
- J.G.S. Marcano, T.T. Tsotsis, *Catalytic Membranes and Membrane Reactors*, Wiley, Weinheim, 2002.
- S.Y. Lim, B. Park, F. Hung, M. Sahimi, T.T. Tsotsis, *Chem. Eng. Sci.* 57 (2002) 4933–4946.
- T. Popken, L. Gotze, J. Gmehling, *Ind. Eng. Chem. Res.* 39 (2001) 2601.
- S. Ishigaki, S. Goto, *J. Chem. Eng. Jpn.* 27 (1994) 309–313.
- P. Samranpiboon, R. Jiraratananon, D. Uttapap, X. Feng, R.Y.M. Huang, *J. Membr. Sci.* 173 (2000) 53–59.
- R.M. Waldburger, F. Widmer, W. Heinzlmann, *Chem. Eng. Tech.* 66 (1994) 850–854.